

# Effect of Permanent Load in Gresik Alluvium on Friction Pile Embedment Depth

James J. Oetomo<sup>1,\*</sup>, Ahmad Sulaiman<sup>2</sup>, Ryan Achmad Fadhillah<sup>3</sup>, Eka Diah Astuti<sup>4</sup>

<sup>1</sup> Senior Geotechnical Engineer, PT JGC Indonesia, Indonesia; james.jatmiko.oetomo@gmail.com

<sup>2</sup> Senior Geotechnical Engineer, PT Soilens, Indonesia; 1995.ahmadsulaiman@gmail.com

<sup>3</sup> Geotechnical Engineer, PT Soilens, Indonesia; ryan.achmad@soilens.com

<sup>4</sup> Structural Engineer, PT JGC Indonesia, Indonesia; ekadiahastuti@gmail.com

\*Correspondence: james.jatmiko.oetomo@gmail.com

SUBMITTED 25 July 2023 REVISED 26 August 2023 ACCEPTED 01 September 2023

**ABSTRACT** Hydrostatic load, approximately 250-35 kPa (i.e., water of 2.5m-3.5m high), has been applied in the project area for about 25 years; hereafter, it will be referred as permanent load. Recently, this permanent load including its perimeter embankment, is demolished for which a new facility will be built. The upper 2-4m soil layer in this area consists of fill soil (mainly cohesionless material) overlying thick Gresik alluvium layer. A bearing layer was not found (down to an investigation depth of 50m). The initial design of pile embedment depth refers to the legacy soil report, pile embedment information from the surrounding area (not being subjected by permanent load), and preliminary soil investigation data (from the surrounding area); in this case, the projected embedment depth is 20-23m with the friction pile design concept. Due to the proximity of project location with existing facilities, the jacking-driven pile method, with HSPD (Hydraulic Static Pile Driver) machine, is selected for installing the precast spun pile. The pile jacking works indicate that piles can only be driven down to a depth of about 12m (far less than the projected depth). This paper provides an analysis on the changes of soil properties due to permanent load, which in turn increasing the pile shaft capacity and effectively reducing the pile embedment depth. The analysis is supported by data from pile jacking record, PDA test, and instrumented test pile. Discussion regarding the conservatism in pile design is also presented.

**KEYWORDS** Gresik Alluvium; Permanent Load; Friction Pile; Jacking pile, press-in piling, pile embedment

## 1 INTRODUCTION

Gresik alluvium soil is a quaternary (Holocene) deposit consisting of cohesive and cohesionless particles with some shell fragments. It covers the northwest side of Gresik city, bounded by anticline Sekarkurung at south Supandjono et al. (1992). The Gresik alluvial deposit is intricately linked with and supplied by the Bengawan Solo river; it is the longest river in Java ( $\pm 600$  km long), with river basin of  $\pm 16100$  km<sup>2</sup> Takeuchi et al. (1995). Nowadays, this river is still actively transporting sediment, notably in the rainy period, of which the sediment concentration can be five times of dry period Soemitro et al. (2022).

The sediment deposition process, which formed the Gresik alluvium, started from late Pleistocene; at that time, Gresik was a coastal region with undulating anticline terrain formed during Plio-Pleistocene and it is mostly under the sea level during early Holocene Moechtar (2021). A microfauna analysis of Gresik alluvium suggests that it was deposited in various neritic zone (shallow part of ocean) and coastal lagoon zone Luga (2009).

The geological map of Bengawan Solo river basin is shown in Figure 1; as it can be seen here, this river streamline intersects with the Holocene alluvium zone. The alluvium deposits stretch from Bojonegoro to Gresik, about 125km long from west to east. Geologically speaking, this alluvium zone fills the Randublatung depression, a transitional zone between Rembang shelf at north and

Kendeng trough at south Darman and Sidi (2000); the latter is known to be geologically active De Genevraye and Samuel (1972).

Until late 19th century, the Bengawan Solo river flows directly to Madura strait; in 1880s, for minimizing strait sedimentation, a channel was built, forcing it to flow north (to Ujung Pangkah), directly into the Java sea Whitten et al. (1996). The area surrounding this channel consists of primarily fish ponds (Figure 2a). However, more recently, some of these has been changed into industrial area (Figure 2b), especially at the northwest part of Gresik city.

A new industrial facility is to be built in the Gresik industrial area, facing the Madura strait; it will sit on Gresik Alluvium soil. A hydrostatic load, approximately 2.5m-3.5m high, has been applied in the project area for approximately 25 years. A concrete slab, 30cm thick was present as part of the containment structure which was supported by 80cm thick limestone fill layer. This was an above ground pond, enclosed by earth embankment. Hereafter, the hydrostatic load, including the containment structure, will be referred as permanent load. This existing facility will be demolished prior to the construction of new facility.

The new facility will be supported on friction pile foundation; reasons for selecting this foundation concept: (1) No traditional hard soil layer (SPT N-value >50) down to a depth of 50m; (2) Soils are not considered soft/loose with SPT N-value in the range of 20-30 (at the upper 30m layer); (3) Pile in the existing facilities used the same design concept. These piles will be installed with jacking (a.k.a. jacked-in) method using HSPD (Hydraulic Static Pile Driver) machine, which is necessary for minimizing noise and vibration impact to surrounding existing facilities.

In this paper, firstly, we describe Gresik alluvium properties from geotechnical perspective; based on data from three (3) soil investigation reports. Influence of permanent load to Gresik alluvium will be discussed. Thereafter, the impact of such permanent load to the pile bearing capacity will be elaborated based pile test data (PDA and instrumented test pile). The associated challenges of designing friction pile in this ground condition will be discussed.

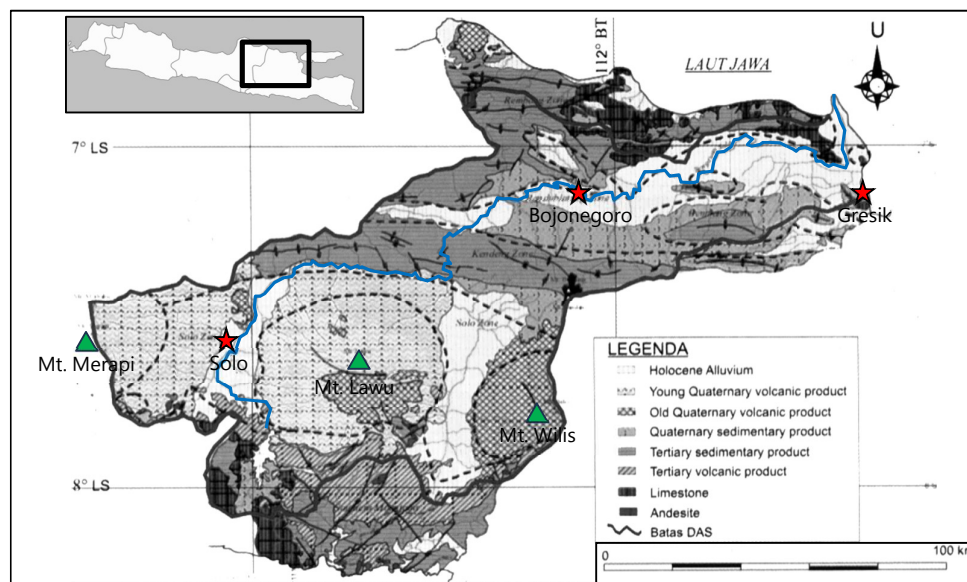


Figure 1. Geological map of Bengawan Solo river basin – Holocene alluvium deposit is lightly-shaded – main Bengawan Solo river line is marked with blue color (adapted from PU SDA (2005))

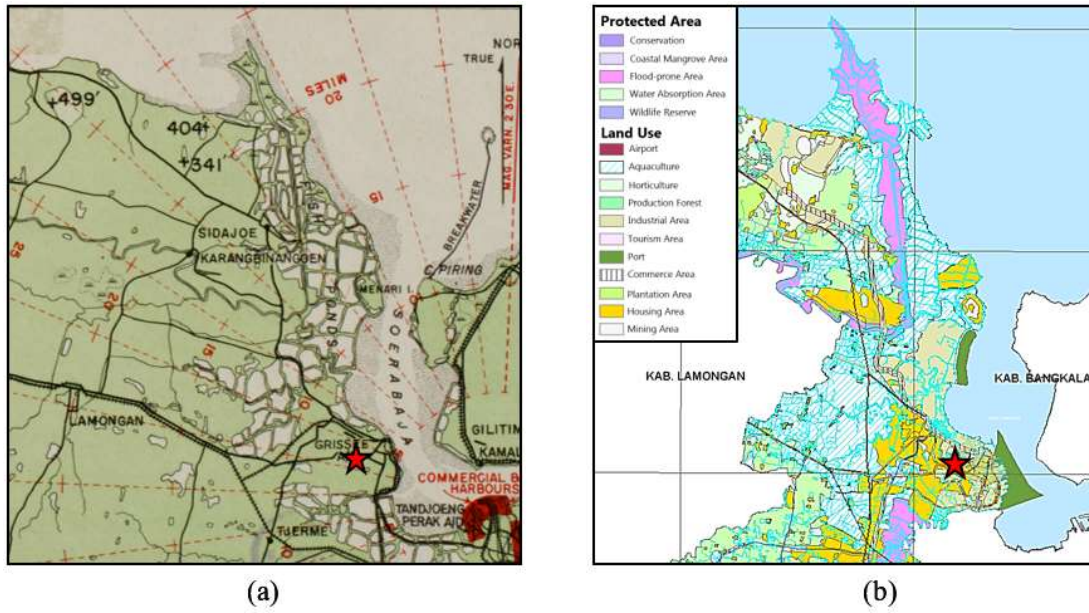


Figure 2. Fish-pond in the surrounding Bengawan Solo diverting channel – at the northwest side of Gresik city (marked with star): (a) Condition about eighty years ago Allied Air Force SWPA (1944); (b) Some fish-pond areas have changed into housing and industrial area DPUTR Gresik (2010)

## 2 SUBSURFACE GROUND DATA

General information of the soil data is given in Table 1; these data are obtained by three (3) different soil investigation companies at different time; therefore, some inherent variations may exist between them. These data are referred as Data A, Data B, and Data C, respectively, classified according to their locations. These soil data are taken from Manyar subdistrict, approximately 3km northward from Gresik city. Data A is the oldest data (1995) and its boreholes (BH) are located approximately 300m away from the actual project location. Data B are taken from points on the perimeter of existing pond facility, while data C represents soil data inside the project area.

Table 1. General information of available soil investigation report in the vicinity of project area

Soil Data	Year	BH Qty	BH Depth	Location
Data A	1995	7 BH	50m (6 BH) 100m (1 BH)	Located approximately 300m from Data B and Data C, farther inland from coastal line
Data B	Early 2021	3 BH	50m	Located at the perimeter of existing pond facility
	Late 2021	1 BH	50m	
Data C	Late 2021	5 BH	50m	Located inside the project area (subjected under permanent load)

SPT N-value comparison of the three mentioned data is shown in Figure 3; Data A vs Data C in Figure 3a and Data B vs Data C in Figure 3b. The upper 2-4m consists of cohesionless fill soil; SPT N-values of this layer are <10 in Data A, but larger in both Data B and Data C (between 10-40). It overlays a very soft thin (2-3m) clay/silt layer with SPT N-value <5; presumably, this is the original alluvial surface layer. The underlying layer consists of silty/clayey sand, approximately 5-15m thick. Generally, from Figure 3, we can note that the area subjected under permanent load (Data C) produces higher SPT N-value, about 5-10 points higher at the upper 25m layer.

The older soil layer (at depth >20-25m) consists of high plasticity stiff clay with some sand lenses; SPT N-values of this layer vary between 20-40, with larger value towards deeper strata. Crushed shells were recorded in some boring logs (Data A and Data B) which were found at depth of 20-50m;

layers containing crushed shell are indicated with marker in Figure 3. Based on the 100m deep borehole in Data A, a hard cemented clay soils with SPT N-value of 40-50 was found at depth of 58m-78m. Thereafter, down to a depth of 100m, the supporting layer consists of very hard cemented clay soil; no rock layer was found at this depth. This is in conformance with the data from Martin (1883), where carbonate rock (marlstone) was only found after a depth of 193.5m.

The plasticity chart of the upper 20m layer shown in Figure 4a indicates that soils in Data A generally have higher plasticity compared to either Data B and Data C. It also shows that the upper 20m soil layer from Data B and Data C is more similar; this is expected, as they are more closely located. The underlying layer consists of primarily high plasticity clay soil (Figure 4b), consistent among the available data. Most of the samples are above the A-Line or just slightly below the A-line, indicating that the fine-grained soil tends to be clay-like. None of the samples is plotted above the U-line, thus the specimen plasticity is well within the known upper plasticity limit.

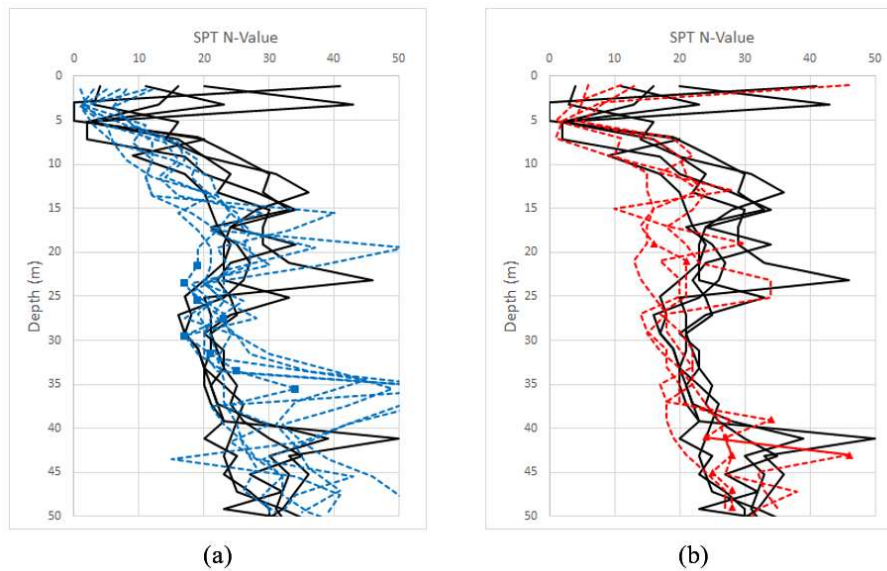


Figure 3. SPT N-value of tested Gresik alluvium samples: (a) Data A in dashed-blue vs Data C in solid-black; (b) Data B in dashed-red vs Data C in solid-black – marker indicates recorded crushed shell at a particular soil layer (from boring log)

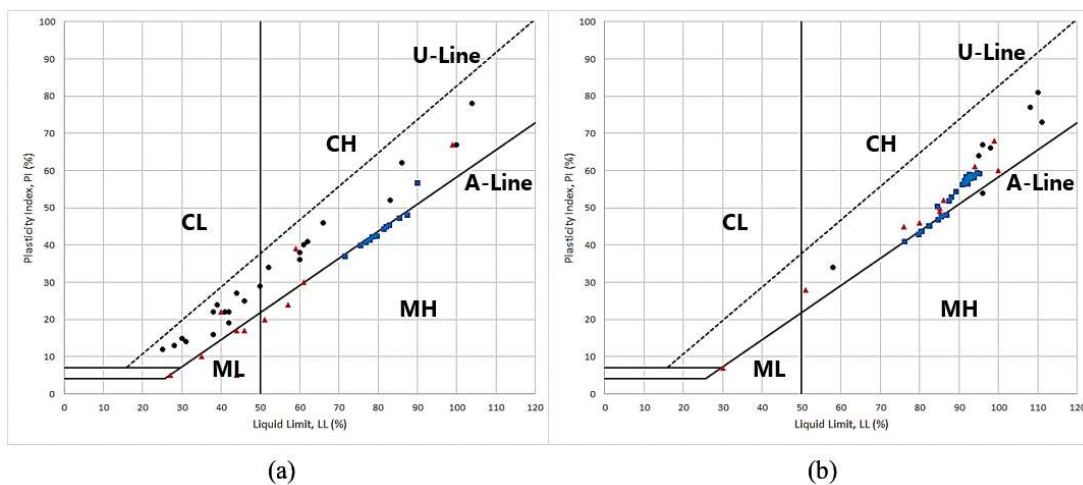


Figure 4. Plasticity chart of tested Gresik alluvium samples: (a) Data from the upper 20m layer; (b) Data from soil depth of 20-50m; Data A = blue rectangle, Data B = red triangle, Data C = black circle

Following up the previously presented plasticity chart, the soil water content and the corresponding liquidity index are shown in Figure 5. The soil water contents (Figure 5a) are mostly hovering around 30%-50%, indicating a fully saturated condition. The liquidity index ( $\frac{w_c - PL}{LL - P}$ ) values are shown in Figure 5b. By comparing Data B and Data C, we can see that liquidity index values in Data C are smaller than Data B; this hints a better soil shear strength in Data C. Indeed, from the literature Skempton and Northey (1952), Leroueil and Tavenas (1983), it is known that lower liquidity index correlates to a higher unconfined compressive strength and vice-versa.

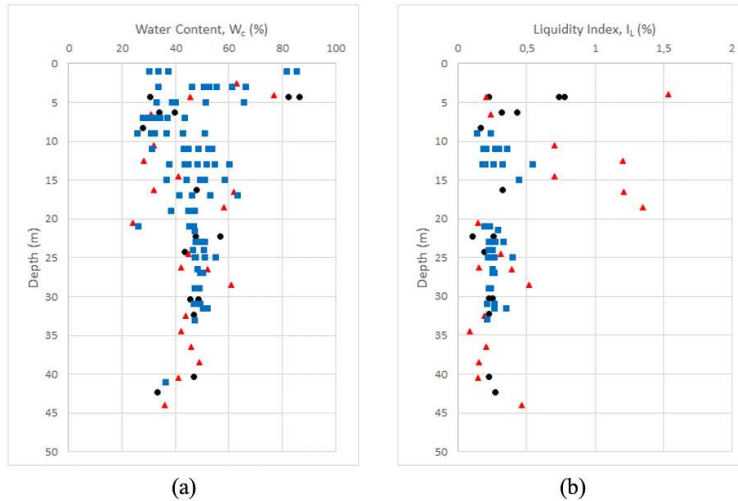


Figure 5. Water content ( $W_c$ ) and liquidity index of tested Gresik alluvium samples – Data A = blue rectangle, Data B = red triangle, Data C = black circle

The fine content for tested samples, in function of depth, is shown in Figure 6. Interestingly, there is a distinct boundary at depth of about 20m; the upper 20m layer contains substantial sand content, while the layer beneath is almost exclusively fine-grained soil. Coincidentally, as previously mentioned, crushed shells were only recorded at those deeper layers. One possible explanation, this location was a downstream deltaic sediment, underneath the then sea level, where fine-grained sediments are prominent. Thereafter, as the seawater transgression ceased post mid-Holocene Highstand (about 6-4.2 ka BP) Sathiamurthy and Voris (2006), sediments may have been accumulated above the sea level, thus basic alluvial fan process such as cut-and-fill Harvey (1984) and coarsening upward Steel (1976) becomes prominent which bring substantial granular deposits at top. The regional tectonic setting would also play a role, but it is not discussed in this paper.

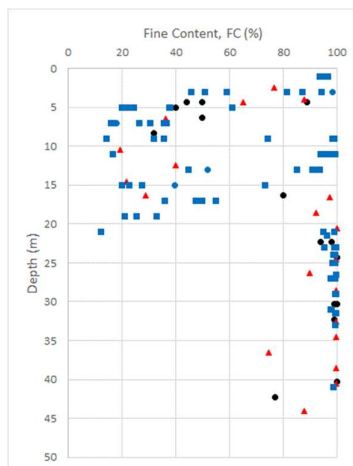


Figure 6. Fine content (percentage of soil passing sieve #200, by weight) of tested Gresik alluvium samples – Data A = blue rectangle, Data B = red triangle, Data C = black circle

In regards of the engineering properties, we present the reported pre-consolidation pressure from consolidation test in Figure 7. The pre-consolidation pressure from Data B and Data C is larger or at the upper bound boundary of Data A. The gap between Data A and Data B/Data C is quite significant, about 50kPa in some cases which can be attributed, at least in some part, to the application of permanent load. Also, it must be noted that the upper soil layer of Data A is inherently slightly different (Figure 4a), such that it may have a lower pre-consolidation pressure in the first place.

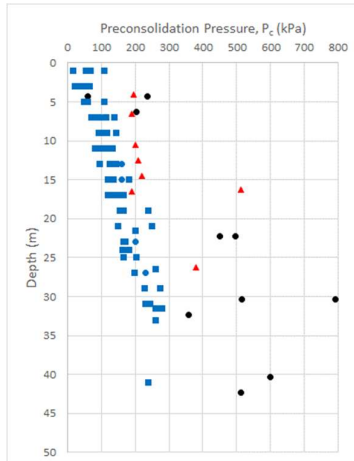


Figure 7. Pre-consolidation pressure of tested Gresik alluvium samples – Data A = blue rectangle, Data B = red triangle, Data C = black circle

### 3 DESIGN OF PILE CAPACITY

The driven pile uses Prestressed Concrete (PC) spun pile, conforming to JIS (1987). The concrete material design compressive strength is 50 MPa. The design of axial pile capacity refers to the API RP-2A recommendation API (2007), using software APILE version 2018. This method is generally known for its conservativeness; hence, it was initially considered the safe approach in the design of friction pile.

In cohesive soil, the pile shaft friction is calculated using the following formula:

$$f_{s,cohesive} = \alpha c \quad (1)$$

where:  $\alpha$  is a dimensionless factor and  $c$  is the soil undrained shear strength. The dimensionless factor  $\alpha$  corresponds to the soil adhesion factor and it is calculated using the following:

$$\begin{aligned} \alpha &= 0.5\psi^{-0.5} \text{ for } \psi \leq 1.0 \\ \alpha &= 0.5\psi^{-0.25} \text{ for } \psi > 1.0 \end{aligned} \quad (2)$$

The parameter  $\psi = c/p'_o$  is the normalized cohesion value with  $p'_o$  is the effective overburden pressure at a particular soil layer. The soil undrained shear strength is correlated from SPT N-value data using  $c = 6.25 \times SPT$ .

For cohesionless soil, the pile shaft friction depends directly on the effective overburden pressure  $p'_o$  and formulated using the following:

$$f_{s,cohesionless} = \beta p'_o \quad (3)$$

where:  $\beta$  is a dimensionless adhesion factor which depends on the cohesionless soil relative density, denser soil has a larger  $\beta$  value.

The pile toe is expected to sit on cohesionless soil, the pile toe unit end bearing capacity is formulated using the following:

$$q = N_q p'_0 \quad (4)$$

with:  $N_q$  is a dimensionless bearing capacity factor.

Figure 8 show the ultimate friction capacity of pile with diameter 450mm, based on Data B and Data C respectively, calculated using borehole data from each data set. The estimated friction capacity seems to be largely equal for both data set at upper subsurface layer of 0-15m; however, the friction capacity of Data C (which is influenced by permanent load) looks subtly larger at depth of 15-30m. The toe capacity is approximately 100-300kN across the shown depth.

The friction pile, in essence, is a depth-controlled pile; thus, a certain design-penetration depth shall be selected such that the followings are met: (1) pile capacity is sufficient for supporting the superstructure load; (2) underlying settlement shall be minimal or as required by design requirement; (3) by considering the selected driving method (jacking in this case), such design-penetration depth shall be attainable. The first and second points are straightforward; however, determining the latter (i.e., design-penetration depth) is tricky in medium stiff soil such as this case. For this reason, the design-penetration depth refers to the known pile embedment depth in the existing facilities, which mostly is in the range of 20-23m; thus, the design-penetration depth is set at 21m. At such depth, the estimated ultimate pile bearing capacity is approximately 1500-1800kN. Using safety factor of 2.5, the allowable pile capacity equals to 600-720kN.

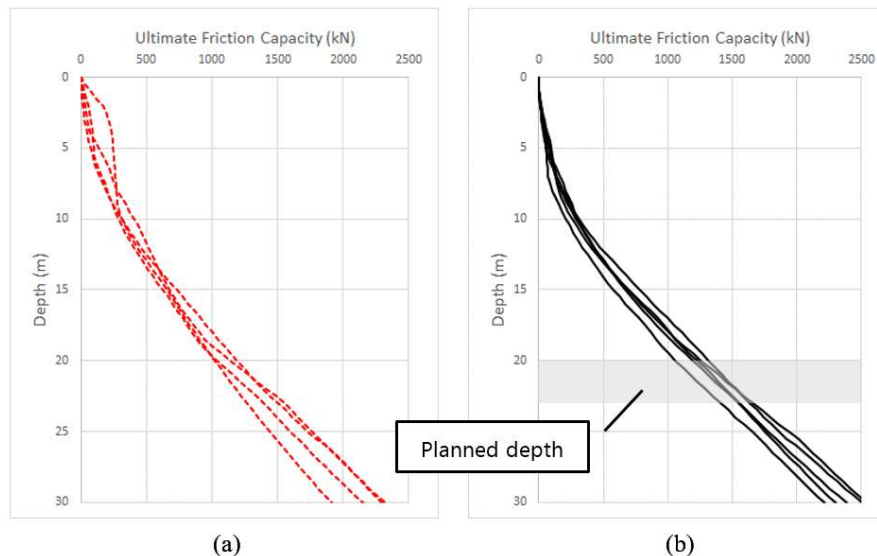


Figure 8. Ultimate friction capacity of pile with diameter 450mm: (a) Data B – dashed line; (b) Data C – solid line

#### 4 PILE DRIVING AND TEST PILE RESULT

For verifying the calculated design capacity, several test piles have been driven in the area previously subjected under permanent load. The driving work would be terminated when the design-penetration depth has been reached or when the measured jacking force exceeds two times (2x) of pile allowable capacity. The actual pile penetration depth is shown in Figure 9; the SPT N-value (from data C) and the measured jacking force data (from HSPD machine) are shown as reference. It can be seen here, qualitatively speaking, their shapes are very similar, indicating the appropriateness of jacking force measurements. However, the actual pile termination depths are only 12-13m, way less than the design-penetration depth of 21m.

Figure 10a shows the pile shaft resistances from PDA (high-strain dynamic) test results from a pile on the perimeter of permanent load area (tested in early 2010s) and piles within the area subjected under permanent load (tested in 2022). The ultimate pile capacities (D450) are between 1500-1850kN; it is in the same range, for both cases (i.e., subjected under and without permanent load). Thus, even with a very different penetration depth, they provide same supporting capacities.

Although the upper fill layer has a substantial penetration resistance (Figure 9), the shaft resistance contribution is minimal. This is as expected because the corresponding effective overburden pressure is low (see Eq. (3)). On the other hand, for the underlying cohesive strata, the permanent load seems to have a noticeable impact, increasing the unit skin resistance (Figure 10b).

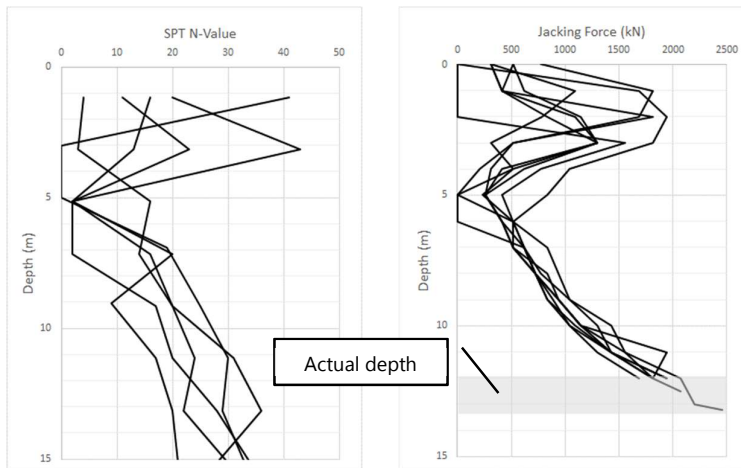


Figure 9. Actual penetration depth of test piles (12-13m); SPT N-value and measured jacking force data are shown as reference

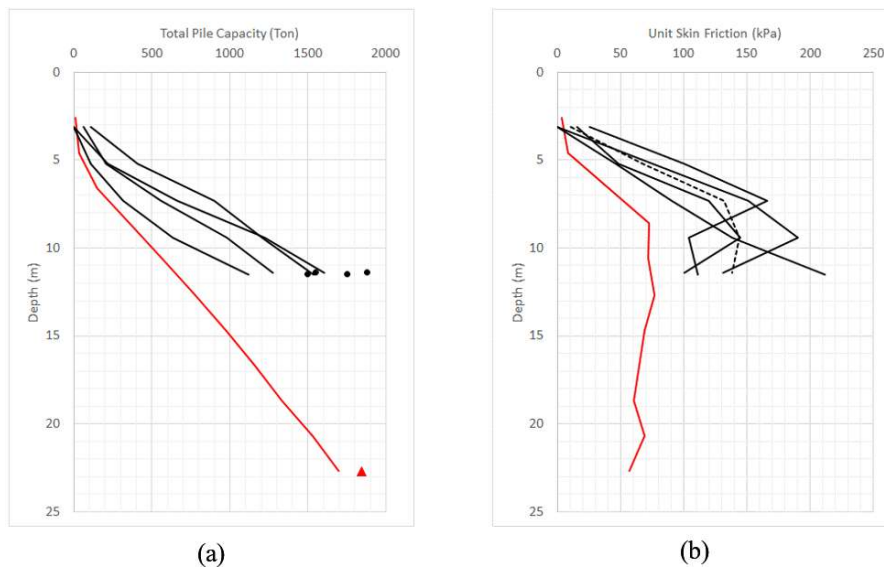


Figure 10. PDA results of D450 piles: (a) Pile shaft capacity in function of depth, marker indicates pile ultimate capacity (after adding toe capacities); (b) Unit friction in function of depth – (red line, triangle marker) Pile test on the perimeter (outside) of permanent load area, tested in early 2010s; (black line, circle marker) Pile test within the area subjected under permanent load, tested in 2022, average value shown with dashed line

One of the tested D450 pile (12m embedment depth) is instrumented where strain gauges are embedded within the PC spun pile so that strains at designated depths can be measured. These strain gauges area installed at depth of 3m, 7m, and 11m from the pile top. Figure 11a shows the calculated mobilized skin resistance during the loading progression; corresponding mobilized unit skin friction is shown in Figure 11b. It must be highlighted that the unit skin friction at deeper depths may have not been fully mobilized; in effect, only mobilized unit skin friction of the upper pile segment would be in a good agreement with PDA test results.

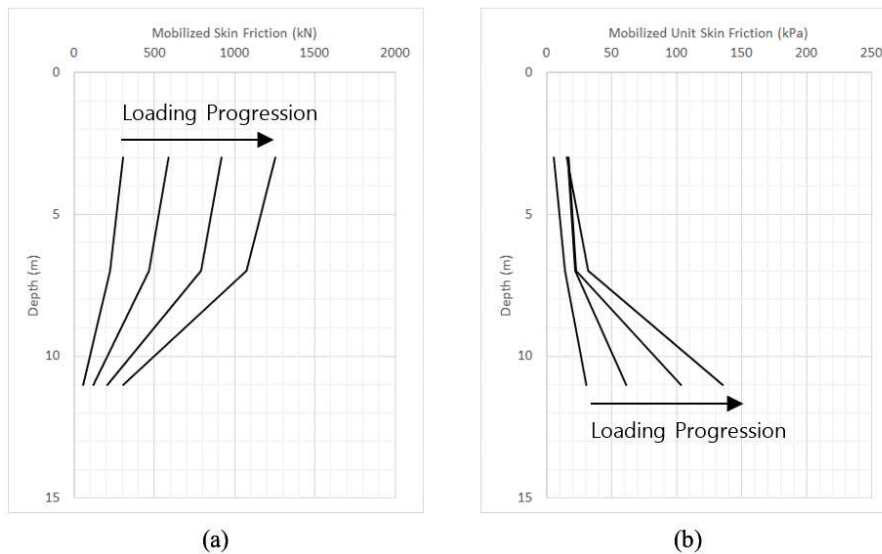


Figure 11. Instrumented pile result of D450 pile: (a) Mobilized skin friction; (b) Mobilized unit skin friction – Loading sequences: 50% (330kN), 100% (660kN), 150% (990kN), and 200% (1320kN)

In view of the above results, we can note the following remarks:

- As previously evoked, under the permanent load, there is little-to-no increase of unit frictional resistance at the upper fill layer. Based on PDA test results, and confirmed by instrumented test pile, it is shown that the unit skin friction of the upper soil layer is only about 15-25kPa.
- For the underlying Gresik alluvium soil, the permanent load increases the soil unit frictional resistance by about 25-50kPa. This can be attributed to the increase of soil adhesion by approximately the same amount (see Eq. (1)).
- Knowing that the estimated permanent load (hydrostatic + concrete + limestone) is equal to  $30+7.2+16 = 53.2$  kPa, then for obtaining the above-mentioned increase of soil unit frictional resistance, the adhesion shall also increase substantially, i.e., by 50%-100% of the applied permanent load across the pile embedment depth.

## 5 CONCLUSION

In this study, properties of Gresik alluvium soil have been described based on three (3) separate soil investigation data, conducted at different times. The upper soil layer (2-4m) consists of fill layer overlying a very soft and thin silt/clay soil (2-3m). The alluvial soil beneath it, consists of silt and clay with noticeable amount of sand, down to a depth of 20m. The deep underlying layer consists of high plasticity clay soil with very limited sand content. The permanent load (water, limestone, concrete paving) from an existing above ground pond facility (approximately 53.2kPa), applied for about 25 years, has increased the soil engineering properties as indicated from: (1) SPT N-value; (2) Liquidity index; (3) Pre-consolidation pressure. The estimated improved depth is about 25-30m.

Friction pile is a depth-controlled pile; hence a design embedment depth shall be selected, meeting the strength, settlement, and drivable. In this case, the friction pile initial design embedment depth is 20-23m, which refers to the known embedment depth in the surrounding facilities (not subjected under permanent load). However, the actual embedment depth within the area subjected under permanent load is only 12-13m, leading to an over-design of pile embedment depth.

After comparing PDA test data from the area subjected under permanent load and without permanent load, we found that the pile unit friction capacity has increased considerably (see Figure 10 and Figure 11). In this case, the estimated increase of soil adhesion is about 50%-100% of the applied permanent load. This is considered a large improvement, compared to the commonly known

improvement ratio of 20%-30% Wu et al. (2021), Djunaidy and Wijaya (2020) in the case of soil improvement with preloading.

In relation with the formula for estimating pile capacity, we can note the following:

- Some of commonly used formula for predicting pile capacity may be overly-conservative. While this is the safe approach (for determining pile capacity); the applied API formula proved to be inherently too conservative as the predicted pile capacity does not sufficiently reflect the improved soil properties at the upper subsurface layer. In this case, the predicted pile capacity (in average) at depth of 13m is only 869kN (Figure 8b) while the actual pile capacity more-or-less doubles this prediction.
- Moreover, shaft capacity formula from API penalizes the increase of cohesion through its form of adhesion factor formula. As an illustration, at depth of 10m, in the original soil condition, with average SPT N-value of 17 (correlated  $c=106.25\text{kPa}$ ), the normalized cohesion value  $\psi$  equals to  $0.5 \left( \frac{106.25}{100} \right)^{-0.25} = 0.49$ , yielding unit shaft friction of 52kPa. Assuming the cohesion increases by 50 kPa (due to permanent load), the unit skin friction (i.e., adhesion) only increases to 70 kPa; which means, only less than half of added cohesion is translated into unit skin friction.

Furthermore, it is also worth discussed whether the reduced embedment depth may have been contributed from the selected pile installation method. In comparison to hammer-driven pile, the load application rate (during driving) in jacking-driven pile is relatively low, hence the instantaneous shaft resistance would be close to the static resistance, as calculated from a closed-form formula; nonetheless, the installation rate will still affect the instantaneous shaft resistance of which larger rate correlates to a smaller instantaneous shaft resistance Jackson et al. (2008). Hence, the pile drivability (i.e., expected embedment depth) of jacking pile relies heavily on the selected closed-form formula for predicting the pile capacity.

While we do not have the information of applied piling method in the existing facility, there is a good possibility that a deeper penetration depth could be attained, if hammer-driven pile was used. Thus, the shorter embedment depth (compared to the projected depth) may have been at least contributed from: (1) increase of soil properties by the application of permanent load and (2) different piling method. A follow-up study of jacking pile drivability may be necessary.

In addition to, the following recommendations are to be considered for the design of friction pile, particularly in medium stiff Gresik alluvium soil:

- Several closed-form formulas for predicting pile capacity shall be used for evaluating the range of estimated pile embedment depth. Unless a more in-depth analysis has been conducted, this is a prudent approach for managing the pile embedment depth expectation.
- While the familiarity with the site and local-knowledge on the pile characteristic is important for predicting the pile capacity as highlighted in Jardine et al. (2001), it should not be relied-upon, which may, in this case, overshadow the known loading history.
- The use of instrumented pile is useful for validating the unit skin friction across the embedment depth. However, knowing that the mobilized skin friction is gradual (from top-to-bottom), then the skin resistance from a deeper layer may have not been fully mobilized. Thus, the test pile should be loaded to failure (typically 300% of allowable pile capacity)

## REFERENCES

Allied Air Force SWPA, 1944. Soerabaja commercial & naval hrbrs map. Koninklijk Instituut voor de Tropen (KIT). <http://hdl.handle.net/1887.1/item:2012583>

API – American Petroleum Institute, 2007. Recommended practice for planning, designing and constructing fixed offshore platforms – working stress design, Chapter 6.3.

- Darman, H., & Sidi, F. H., 2000. An outline of the geology of Indonesia, Chapter 4.2. Indonesian Association of Geologist.
- Djunaidy, M. W., & Wijaya, A. E., 2020. Aplikasi vacuum consolidation method pada pengembangan kawasan perumahan di utara Jakarta. HATTI Geotalk XI, 5 May 2020.
- DPUTR (Dinas Pekerjaan Umum & Tata Ruang) Gresik, 2010. Pemutakhiran dan penyerasian analisis dan perencanaan tata ruang wilayah (RTRW) Kabupaten Gresik. <https://geodatabase.gresikkab.go.id/dokumen>
- de Genevraye, P., & Samuel, L., 1972. Geology of the Kendeng zone (central and east Java). Proceedings of Indonesian Petroleum Association 1st Annual Convention.
- Harvey, A. M., 1984. Aggradation and dissection sequences of Spanish alluvial fans: influence on morphological development. *Catena*. 11(1), pp. 289-304. [https://doi.org/10.1016/S0341-8162\(84\)80027-2](https://doi.org/10.1016/S0341-8162(84)80027-2)
- Jackson, A. M., White, D. J., Bolton, M. D., & Nagayama, T., 2008. Pore pressure effects in sand and silt during pile jacking. Proceedings of the BGA International Conference on Foundations, Dundee, Scotland, 24-27 June 2008.
- Jardine, R. J., Standing, J. R., Jardine, F. M., Bond, A. J. & Parker, E., 2001. A competition to assess the reliability of pile prediction methods. International conference on soil mechanics and geotechnical engineer, pp. 911-914.
- JIS – Japanese Industry Standard, 1987. JIS A5335 Pretensioned spun concrete piles.
- Leroueil, S. & Tavenas, F., 1983. Propriétés caractéristique des argiles de l'est du Canada. *Canadian Geotechnical Journal*, 20(4), pp. 681-705. <https://doi.org/10.1139/t83-076>
- Lugra, I. W., 2009. Lingkungan pengendapan sedimen di perairan Gresik, Jawa Timur, berdasarkan analisis mikrofauna dari contoh pemboran inti (in Indonesian). *Buletin Sumber Daya Geologi*, 4(3), pp. 33-42.
- Martin, K., 1883. Palaeontologische ergebnisse von tiefbohrungen auf Java, nebst allgemeineren studien ueber das Tertiaer von Java, Timor und Einiger anderer inseln – Paleontological results of deep wells on Java, and more general studies on the Tertiary of Java, Timor and some other islands. *Sammlungen des Geologischen Reichs-Museums in Leiden. Serie 1, Beiträge zur Geologie Ost-Asiens und Australien*, 3(1), pp. 339-349.
- Moechtar, R. A. T., 2021. The dynamics of Holocene sedimentary depositional process in downstream of Bengawan Solo river and tidal zone in Gresik and surrounding areas, East Java (in Indonesian). *Journal of Geology and Mineral Resources*, 22(1), pp. 9-23. <https://doi.org/10.33332/jgsm.geologi.v22i1.553>
- PU SDA (Departemen Pekerjaan Umum, Badan Penelitian dan Pengembangan Pusat Penelitian dan Pengembangan Sumber Daya Air), 2005. Katalog sungai di Indonesia Volume 1.
- Sathiamurthy, E., & Voris H. K., 2006. Maps of Holocene sea level transgression and submerged lakes of the Sunda Shelf. *The Natural History Journal of Chulalongkorn University*, 2, pp. 1-44.
- Skempton, A.W., & Northey R. D., 1952. The sensitivity of clays. *Géotechnique*, 3(1), pp. 30-53. <https://doi.org/10.1680/geot.1952.3.1.30>
- Soemitro, R., Mukunoki, T., Maulana, M., Soetanto, R., Warnana, D. D., & Satrya, T., 2022. Morphology changes affected by sedimen concentration and river flow in meandering channels of the Bengawan Solo river. *Authorea*. <https://doi.org/10.22541/au.166065123.31791213/v1>

---

Steel, R. J., Naehle, S., Nilsen, H. & Roe, S. L., 1976. Coarsening-upward cycles in the alluvium of Hornelen Basin (Devonian) Norway: Sedimentary response to tectonic events.

Geological Society of America Bulletin. 88(8), pp. 1124-1134. [https://doi.org/10.1130/0016-7606\(1977\)88%3C1124:CCITAO%3E2.0.CO;2](https://doi.org/10.1130/0016-7606(1977)88%3C1124:CCITAO%3E2.0.CO;2)

Supandjono, J.B., Hasan, K., Panggabean, H., Satria D., & Sukardi., 1992. Geological map of the Surabaya & Sapulu quadrangle, Jawa. Pusat penelitian dan pengembangan geologi.

Takeuchi, K., Jayawardena, A. W. & Takahasi, Y., 1995. Catalogue of rivers for Southeast Asia and the Pacific – Volume 1. UNESCO-IHP regional steering committee for Southeast Asia and the Pacific.

Whitten, T., Soeriaatmadja, R. E., & Afiff, S. A., 1996. The ecology of Java and Bali.

Wu, J., Xuan, Y., Deng, Y., Li, X., Zha, F., & Zhou, A., 2021. Combined vacuum and surcharge preloading method to improve Lianyungang soft marine clay for embankment widening project: A case. *Geotextiles and Geomembranes*, 49(2), pp. 452-465. <https://doi.org/10.1016/j.geotexmem.2020.10.013>.